

MANIFESTATIONS OF STRONG ELECTROWEAK SYMMETRY BREAKING IN e^-e^- SCATTERING

FRANK CUYPERS

`cuypers@mppmu.mpg.de`

*Max-Planck-Institut für Physik, Werner-Heisenberg-Institut,
D-80805 München, Germany*

Abstract

We analyze the incidence on polarized e^-e^- scattering of the trilinear and quartic anomalous gauge couplings which arise in the realm of a non-linear realization of electroweak symmetry breaking.

1 Introduction

The tree-level gauge couplings in the standard model are dictated by the gauge principle. Deviations from this expectation can arise from several sources, including quantum corrections, new particles or compositeness. Since the standard model quantum corrections are expected to be small [1], such deviations would provide stringent evidence for new physics. Unfortunately, the present experimental bounds still lack by far the accuracy necessary to detect any effect. Dramatic improvements, though, are expected from LHC [2] or the next generation of linear colliders operated in the e^+e^- [3], $e^-\gamma$ and $\gamma\gamma$ [4] or e^-e^- [5, 6] modes.

We consider here a heavy Higgs scenario, where the electroweak symmetry breaking sector is strongly coupled [7]. Chiral perturbation theory enables us to write an effective lagrangian in which the symmetry breaking pattern is fixed by a custodial $SU(2)_c$ global symmetry. The heavy (or even non-existent) Higgs is then seen through an infinite tower of operators, of which only those of lowest order in a momentum expansion contribute to the low energy effective theory. The coefficients of these operators parametrize the unknown physics, which by assumption lies outside the reach of direct investigations. In the unitary gauge, the standard model lagrangian is then supplemented by the following effective lagrangians [2, 3]:

$$L_T = -i \frac{e^3}{32\pi^2 s_w^2} \left[L_{9R} \left(W_\mu^\dagger W_\nu A^{\mu\nu} - \frac{s_w}{c_w} W_\mu^\dagger W_\nu Z^{\mu\nu} \right) + L_{9L} \left(W_\mu^\dagger W_\nu A^{\mu\nu} + \frac{c_w}{s_w} W_\mu^\dagger W_\nu Z^{\mu\nu} + \frac{1}{s_w c_w} (W_{\mu\nu}^\dagger W^\mu - W_{\mu\nu} W^{\dagger\mu}) Z^\nu \right) \right] \quad (1)$$

$$L_Q = \frac{e^4}{32\pi^2 s_w^4} \left[L_1 \left(2(W^\dagger \cdot W)^2 + \frac{2}{c_w^2} (W^\dagger \cdot W) Z \cdot Z + \frac{1}{2c_w^2} (Z \cdot Z)^2 \right) + L_2 \left((W^\dagger \cdot W)^2 + |W \cdot W|^2 + \frac{2}{c_w^2} (W^\dagger \cdot W) Z \cdot Z + \frac{1}{2c_w^2} (Z \cdot Z)^2 \right) \right], \quad (2)$$

where $W_{\mu\nu} = \partial_\mu W_\nu - \partial_\nu W_\mu$ and $V_{\mu\nu} = \partial_\mu V_\nu - \partial_\nu V_\mu$ ($V = \gamma, Z$).

The lagrangian L_T describes anomalous trilinear interactions among the gauge bosons, whereas L_Q modifies the quartic couplings. The latter is also responsible for a new type of $ZZZZ$ interaction, which is absent in the standard model.

It should be remembered that the coefficients L_{9L} , L_{9R} , L_1 and L_2 of the anomalous operators are no fundamental constants, but merely energy-dependent form factors. Moreover, the operators responsible for L_T typically originates from loops, whereas L_Q can be generated at tree-level [8]. Therefore, the natural expectation is that the coefficients L_{9L} and L_{9R} are small compared to L_1 and L_2 . Note also that the operators from which L_T is derived induce quartic terms as well. These, however, should be small compared to the “genuine” quartic anomalies of L_Q , because of the argument given above. We therefore ignore them from now on.

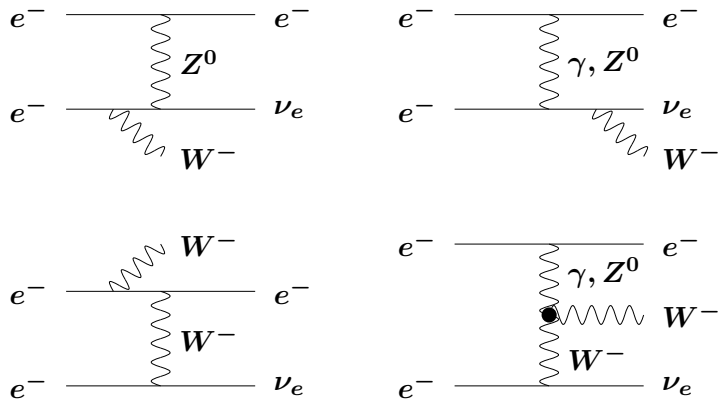


Figure 1: Typical lowest order Feynman diagrams participating to W^- production in e^-e^- scattering.

We analyze here how the addition of the pieces (1,2) to the standard model lagrangian modifies the latter’s predictions in e^-e^- scattering. For this we examine the W^- and W^-Z^0 production reactions, which respectively probe the trilinear and quartic gauge couplings.

2 Trilinear Couplings

In e^-e^- scattering the trilinear anomalous couplings L_{9L} and L_{9R} appear to lowest order in the reaction

$$e^-e^- \rightarrow e^-\nu_e W^- . \quad (3)$$

The Feynman diagrams contributing to this process are depicted in Fig. 1. It is the last diagram, whose trilinear vertex is emphasized, which provides the signals we intend to test. If both electron beams are right-polarized the process does not take place, because at least one of the fermion lines is connected to a W boson. For the LR combination of initial helicities, the third diagram in which a W is exchanged between the two fermion lines, does not contribute. For the LL configuration, all diagrams contribute.

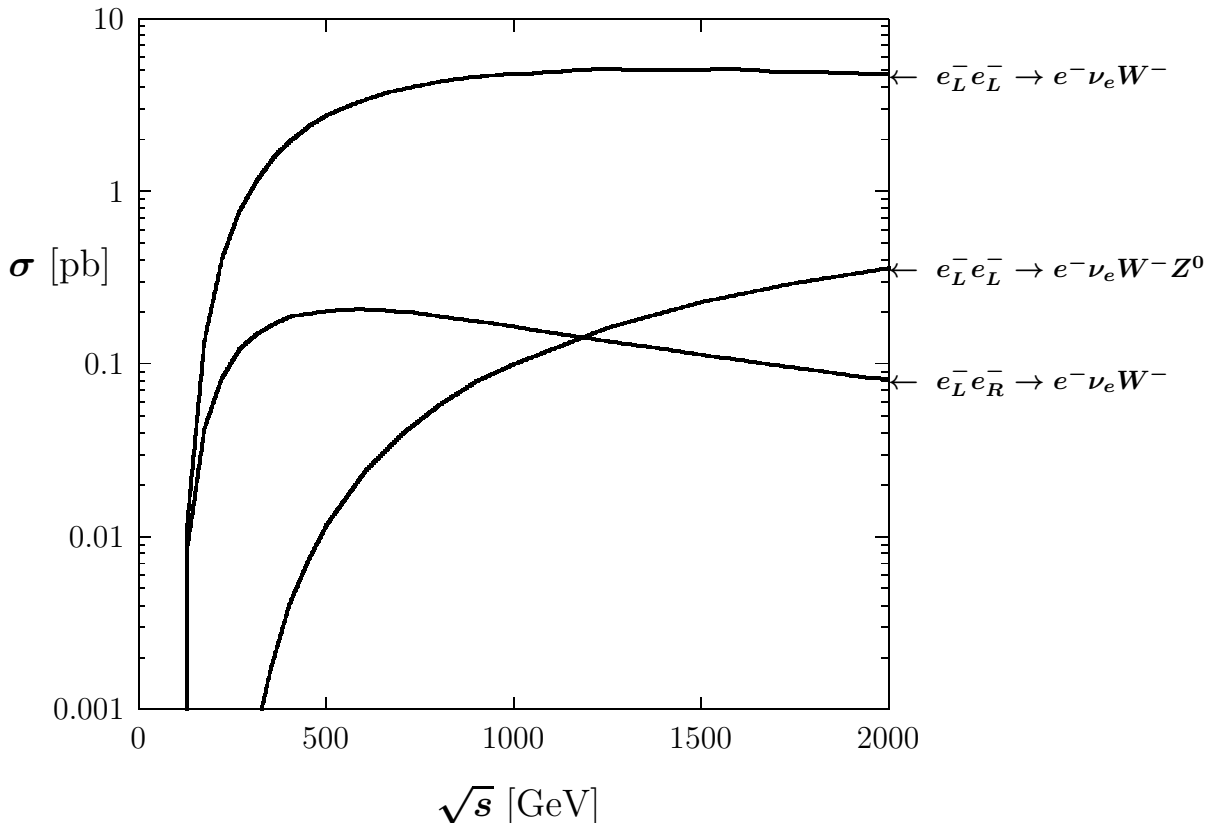


Figure 2: Energy dependence of the polarized W^- production cross sections considered in the text.

To make sure these and only these $e^-\nu_e W^-$ events are seen, we impose the fol-

lowing cuts on the final state:

$$\begin{array}{l}
 \theta_e > 10^\circ \\
 E_e > 10 \text{ GeV} \\
 p_\perp^{\text{vis}} > 10 \text{ GeV} \\
 \text{efficiency} = \frac{2}{3} \quad \Leftarrow \quad \text{only hadronic decays of the } W .
 \end{array} \quad (4)$$

When combined with the measurement of the jets invariant mass, the restriction to only hadronic decays of the W insures the absence of non-resonant backgrounds. Similarly, the requirement of an imbalance in the transverse momentum guarantees that no photoproduction events with only one electron lost along the beam pipe are included. The expected standard model cross sections [5] are displayed as functions of the center of mass energy in Fig. 2. In all calculations we ignore the electron mass, as it is justified at the energies considered with the cuts (4).

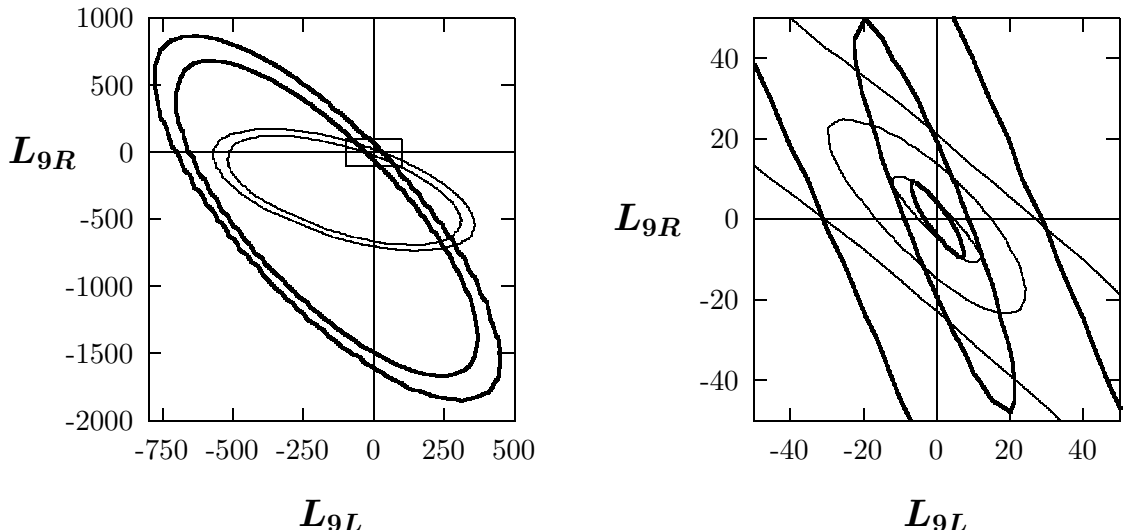


Figure 3: Contours of detectability at 95% confidence for the trilinear anomalous couplings in the polarized $e^-e^- \rightarrow e^-\nu_e W^-$ reactions, with the center of mass energy $\sqrt{s} = 500$ GeV and the luminosity $\mathcal{L} = 20 \text{ fb}^{-1}$. The thin curves are for the LR combination of initial electron polarizations, whereas the thick curves are for the LL combination. The outer to inner contours correspond to the three different analysis described in the text. The plot on the right is a zoom into the boxed region of the left plot.

To determine the discovery potential of the reaction (3) we have used least squares estimators as in Ref. [5]. Assuming there is no anomalous coupling, we explore this way the region around $L_{9L} = L_{9R} = 0$ for the finite values of these parameters which can be excluded with 95% confidence ($\chi^2 \geq 6$). We have performed this analysis with three procedures of increasing resolving power:

1. Using only the information from the total cross sections. As we shall see, this is totally inadequate.
2. Adding information from the differential cross sections, by subdividing the emerging electron's polar angle range into 20 bins for the *LL* case and 10 bins for the *LR* case. This way each bin is guaranteed to contain a sufficiently large number of nearly gaussian distributed events.
3. Computing the Cramer-Rao limit of this reaction [9]

$$\chi^2_\infty = \mathcal{L} \int d\Omega \frac{(\Delta d\sigma/d\Omega)^2}{d\sigma/d\Omega} , \quad (5)$$

where $d\Omega$ is the element of phase space. The resulting bounds on the parameters are the best one may hope to ever achieve with a given luminosity \mathcal{L} in a perfect experiment. They may therefore serve as a benchmark of the reaction.

The number of events is calculated assuming a typical integrated design luminosity scaling like $\mathcal{L} = 80\text{s fb}^{-1}/\text{TeV}$. Since the polar angle of an electron should be measurable to an accuracy better than 10 mrad, the main systematic errors originate from the luminosity measurement and from detector inefficiencies. None of these should exceed 1%, and we conservatively assume an overall systematic uncertainty of 2%.

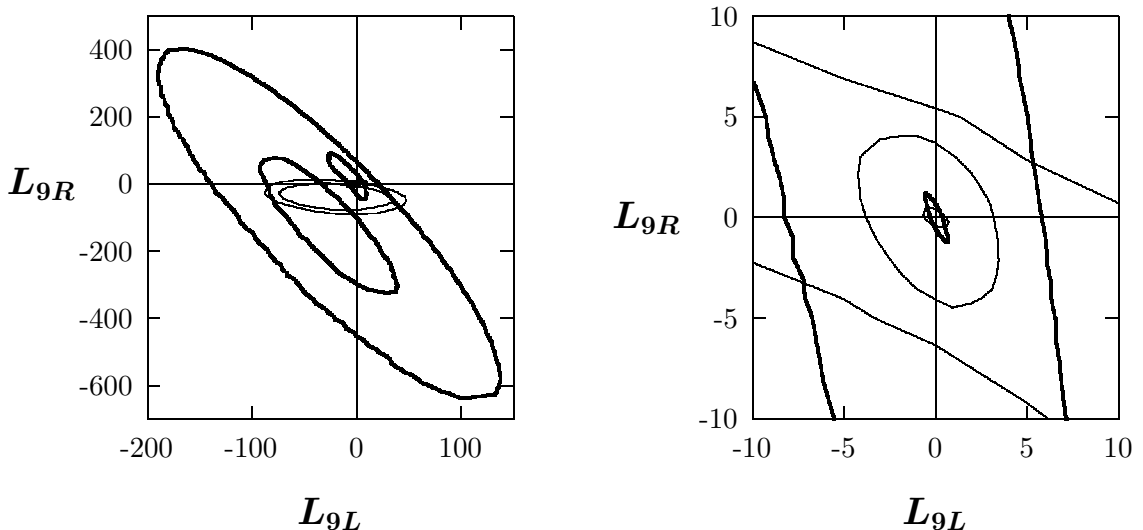


Figure 4: Same as Fig. 3, with $\sqrt{s} = 2$ TeV and $\mathcal{L} = 320 \text{ fb}^{-1}$.

In the second analysis, instead of the electron's polar angle one could as well have chosen another variable, such as the polar angles of the W^- or the ν_e , or the energy or transverse momentum of any combination of the particles. As it turns out, the polar angle of the W^- is actually a more sensitive variable, but it cannot be measured as precisely as the angle of the electron.

In Figs 3 and 4 we have plotted the 95% observability contours of L_{9L} and L_{9R} which can be obtained in 500 GeV and 2 TeV center of mass collisions with each of the three procedures. The information from the total cross section is clearly not sufficient, since it cannot resolve an ambiguity along a closed curve in these two parameters. Taking into account the electron's angular correlations, though, improves the resolution dramatically and totally lifts the ambiguity¹. There may, however, be much more to be gained by using improved observables and multivariate correlations or a maximum likelihood fitting, since the theoretical Cramer-Rao limit of this reaction is still doing better by several factors of one.

It is worth noting that although the standard model cross sections for the LR combination of beam polarizations are much less than those of the LL combination, this experiment can provide better bounds on the parameters. Indeed, the large cross sections of the LL mode are also due to the many more background diagrams. The resolving power of a reaction is not necessarily related to the standard model rates.

3 Quartic Couplings

As we mentioned in the introduction, the L_1 and L_2 quartic anomalous couplings are expected to be larger than the trilinear anomalies L_{9L} and L_{9R} . In a first approximation, it is thus safe to ignore the latter when it comes to study the former. They can be tested to lowest order in the reactions

$$e^- e^- \rightarrow W^- W^- \nu_e \nu_e \quad (6)$$

$$W^- Z^0 \nu_e e^- \quad (7)$$

$$Z^0 Z^0 e^- e^- \quad (8)$$

$$W^+ W^- e^- e^- . \quad (9)$$

It turns out that is the most sensitive process to L_1 and L_2 is the second one (7), with both initial electron beams left polarized [6]. We therefore concentrate solely on this reaction from now on. The 15 topologies of the 88 Feynman diagrams participating to this reaction in the unitary gauge are shown in Fig. 5. It is the last diagram, whose quartic vertex is emphasized, which provides the signals we wish to test.

The expected standard model cross sections [10] are displayed as functions of the center of mass energy in Fig. 2, with the same cuts (4) as in the analysis of the trilinear couplings, except that in order to satisfy the requirement that all events be fully reconstructible, the efficiency drops to approximately 51%. Still, substantial event rates are expected at high energy.

Here again, we estimate the discovery potential of the reaction (7) with the help of a least squares estimator. As in the analysis of the trilinear couplings, we assume a 2% systematic error in this experiment too. Because statistics are lower, though, we

¹ Note that a two-fold ambiguity always subsists when L_{9L} and L_{9R} are probed with the $e^+ e^- \rightarrow W^+ W^-$ reaction.

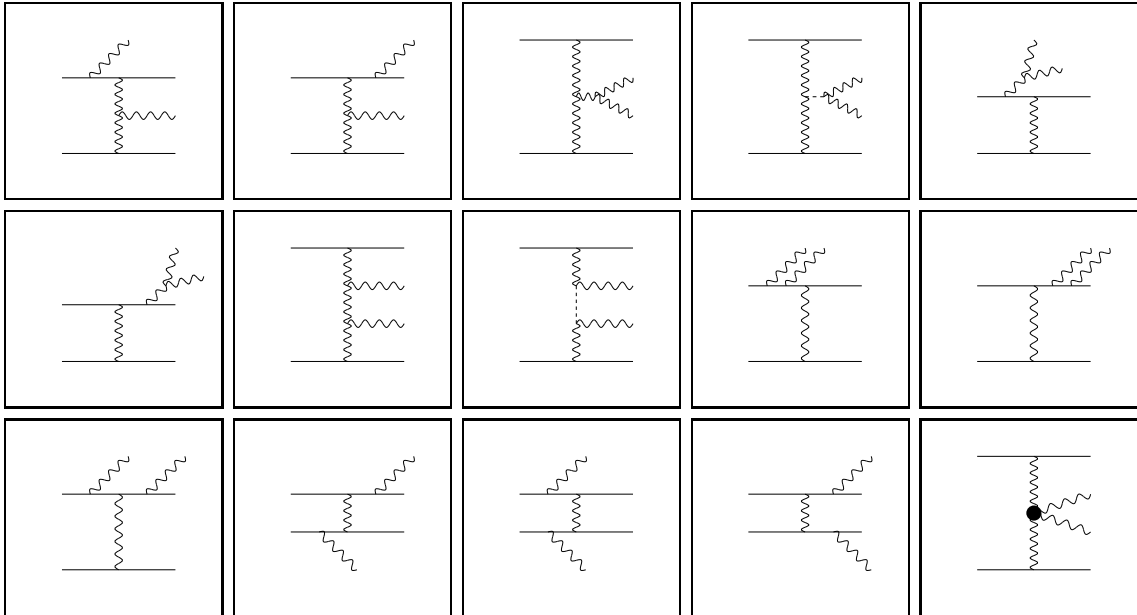


Figure 5: Topologies of the Feynman diagrams for the reaction $e^-e^- \rightarrow W^-Z^0\nu_e e^-$.

refrain from binning the data and only use the total cross section. Since modifications to the quartic couplings destroy the very subtle and powerful unitarity cancellations which in the standard model render the cross section well behaved, this simple minded observable may after all be rather efficient. More work, though, should be performed in this direction to confirm this working hypothesis. Especially at higher energies, where statistics become good, the study of differential distributions may significantly improve these results.

The results of the analysis are plotted in Fig. 6 as the contours around the standard model expectation beyond which the quartic anomalous couplings L_1 and L_2 can be excluded with 95% confidence in the absence of a signal. Expectations are shown for 500 and 2000 GeV center of mass energies.

4 Conclusions

We have analyzed the indirect effects of a strongly interacting Higgs sector in e^-e^- scattering, and find that W^- production is sensitive to the dominant anomalous trilinear and quartic gauge couplings. The resolving power of these reactions is comparable to the one expected from e^+e^- , $e^-\gamma$ or $\gamma\gamma$ experiments when a similar analysis is performed [5, 6].

The sensitivity to the anomalous couplings increases substantially with the collider energy, but a careful choice of sensitive observables remains essential in order to obtain

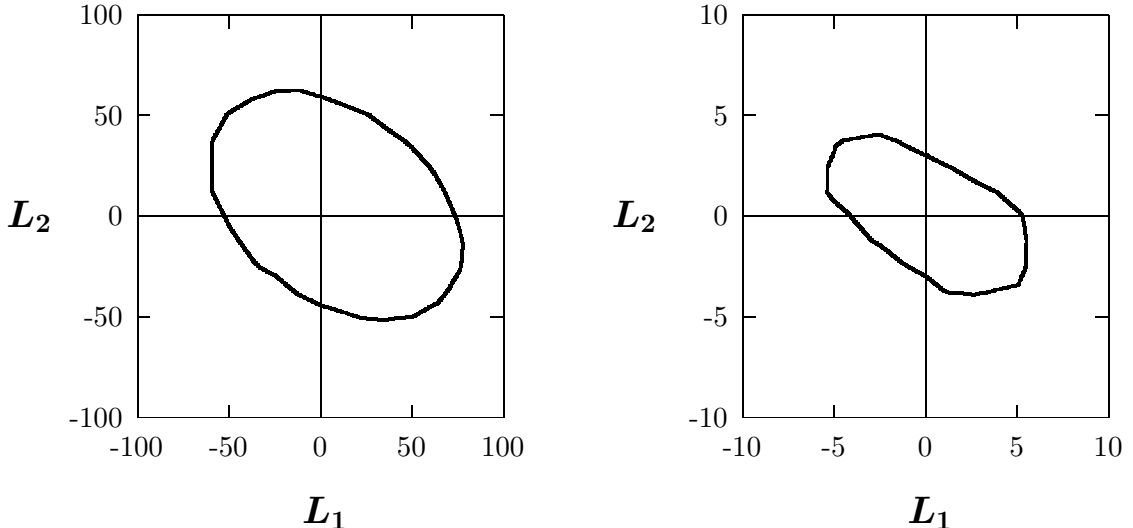


Figure 6: Contours of detectability at 95% confidence for the quartic anomalous couplings in the $e_L^- e_L^- \rightarrow e^- \nu_e W^- Z^0$ reaction. The left plot is obtained for the center of mass energy $\sqrt{s} = 500$ GeV and the luminosity $\mathcal{L} = 20 \text{ fb}^{-1}$, whereas the right plot is obtained with $\sqrt{s} = 2 \text{ TeV}$ and $\mathcal{L} = 320 \text{ fb}^{-1}$.

performing bounds. Such optimizations, including more elaborate treatments of the final states, have been shown to dramatically improve the resolving power of the e^+e^- reactions [3]. They are still to be performed for the e^-e^- processes, but there is no doubt that there is a lot of room for improvement here too.

There were only four independent anomalous couplings involved in this study, because we restricted ourselves to a heavy Higgs scenario. If we relax this assumption and settle for no less than any kind of new physics at the TeV scale, a much larger number of anomalies must be considered, about twelve of lowest dimensions. Having this in mind, it becomes clear that a single experiment is not sufficient to disentangle the complicated interdependences of all the parameters. Therefore, although none of the different e^+e^- , e^-e^- , $e^-\gamma$ or $\gamma\gamma$ linear collider operating modes is clearly performing better than the others in probing anomalous couplings, it will be important to gather as much information as possible from all these experiments in order to obtain the best resolution.

Acknowledgements

It is a pleasure to thank Debajyoti Choudhury and Karol Kołodziej for their collaboration on similar topics.

References

[1] G. Couture *et al.*, *Phys. Rev.* **D36** (1987) 859.

- [2] A.F. Falk, M. Luke, E. H. Simmons, *Nucl. Phys.* **B365** (1991) 523; J. Bagger, S. Dawson, G. Valencia, *Nucl. Phys.* **B399** (1993) 364 and references therein.
- [3] F. Boudjema *et al.*, Proc. of the Workshop *e^+e^- collisions at 500 GeV*, Munich/Annecy/Hamburg, 1992-93, Ed. P. Zerwas and references therein.
- [4] S.Y. Choi, F. Schrempp, *Phys. Lett.* **B272** (1991) 149; E. Yehudai, *Phys. Rev.* **D44** (1991) 3434.
- [5] D. Choudhury, F. Cuypers, *Nucl. Phys.* **B429** (1994) 33 [hep-ph/9405212]; *Phys. Lett.* **B325** (1994) 500 [hep-ph/9312308].
- [6] F. Cuypers, K. Kołodziej, *Phys. Lett.* **B344** (1995) 365 [hep-ph/9411277].
- [7] M. Lüscher, P. Weisz, *Phys. Lett.* **B212** (1989) 472.
- [8] C. Arzt, M.B. Einhorn, J. Wudka, *Nucl. Phys.* **B433** (1995) 41 [hep-ph/9405214].
- [9] F. Cuypers, Proc. of the Workshop *Perspectives for Electroweak Interactions in e^+e^- Collisions* Schloß Ringberg, 1995, World Scientific, Ed.: B. Kniehl [hep-ph/9503252].
- [10] F. Cuypers, K. Kołodziej, R. Rückl, *Nucl. Phys.* **B430** (1994) 231 [hep-ph/9405421]; *Phys. Lett.* **B325** (1994) 243 [hep-ph/9312308].